


Near-future forest vulnerability to drought and fire varies across the western United States

Polly C. Buotte¹  | Samuel Levis² | Beverly E. Law¹  | Tara W. Hudiburg³ | David E. Rupp⁴ | Jeffery J. Kent³

¹Department of Forest Ecosystems, and Society, Oregon State University, Corvallis, Oregon

²SLevis Consulting, LLC, Oceanside, California

³Department of Forest, Rangeland, and Fire Sciences, University of Idaho, Moscow, Idaho

⁴College of Earth, Ocean, and Atmospheric Sciences, Oregon State University, Corvallis, Oregon

Correspondence

Polly C. Buotte, Department of Forest Ecosystems, and Society, Oregon State University, Corvallis, OR.
Email: pcbuotte@gmail.com

Funding information

US Department of Agriculture National Institute of Food and Agriculture; US Department of Energy, Grant/Award Number: DE-FG02-07ER64361; National Science Foundation

Abstract

Recent prolonged droughts and catastrophic wildfires in the western United States have raised concerns about the potential for forest mortality to impact forest structure, forest ecosystem services, and the economic vitality of communities in the coming decades. We used the Community Land Model (CLM) to determine forest vulnerability to mortality from drought and fire by the year 2049. We modified CLM to represent 13 major forest types in the western United States and ran simulations at a 4-km grid resolution, driven with climate projections from two general circulation models under one emissions scenario (RCP 8.5). We developed metrics of vulnerability to short-term extreme and prolonged drought based on annual allocation to stem growth and net primary productivity. We calculated fire vulnerability based on changes in simulated future area burned relative to historical area burned. Simulated historical drought vulnerability was medium to high in areas with observations of recent drought-related mortality. Comparisons of observed and simulated historical area burned indicate simulated future fire vulnerability could be underestimated by 3% in the Sierra Nevada and overestimated by 3% in the Rocky Mountains. Projections show that water-limited forests in the Rocky Mountains, Southwest, and Great Basin regions will be the most vulnerable to future drought-related mortality, and vulnerability to future fire will be highest in the Sierra Nevada and portions of the Rocky Mountains. High carbon-density forests in the Pacific coast and western Cascades regions are projected to be the least vulnerable to either drought or fire. Importantly, differences in climate projections lead to only 1% of the domain with conflicting low and high vulnerability to fire and no area with conflicting drought vulnerability. Our drought vulnerability metrics could be incorporated as probabilistic mortality rates in earth system models, enabling more robust estimates of the feedbacks between the land and atmosphere over the 21st century.

KEYWORDS

climate change, drought, fire, forest, modeling, western United States

1 | INTRODUCTION

Forests in the western United States support high species diversity (Halpern & Spies, 1995; Kline et al., 2016) and include some of the highest carbon-density forests on earth (Law & Waring, 2015; Law et al., 2018). Some of these forests are under increasing stress from accelerated rates of drought-related mortality (Allen et al., 2010; Anderegg et al., 2015; van Mantgem et al., 2009) and wildfires (Littell, McKenzie, Peterson, & Westerling, 2009), bringing urgency to the question of where are forests likely to be most vulnerable to mortality under future climate and atmospheric carbon dioxide concentrations. The ability to simulate forest mortality in this region over the next several decades is critical for assessing forest management strategies—including climate change mitigation, wildfire risk reduction, and habitat preservation strategies—and the potential feedbacks between the land and atmosphere (Bonan & Doney, 2018).

Earth system models (ESMs) have the potential to provide projections of forest vulnerability to mortality. However, the land surface components of most ESMs currently include limited, if any, representation of drought-related forest mortality (McDowell et al., 2011). Quantification of drought-related mortality is essential for estimating future carbon cycling and climate feedbacks (Bonan, 2008), but progress has been limited because of incomplete understanding of the mechanisms involved (McDowell et al., 2008; Sala, Piper, & Hoch, 2010). However, species hydraulic traits explain patterns of recent tree mortality (Anderegg et al., 2016), and there is empirical evidence that both short-term and prolonged drought influence tree mortality (Kane & Kolb, 2014; Macalady & Bugmann, 2014) in the western United States. Most land surface components of ESMs are "big leaf" models in which individual trees are not represented. Therefore, we need to investigate how well this class of models can identify the conditions under which trees are more likely to die (Anderegg, Berry, & Field, 2012).

To address these limitations, our objectives are to modify the Community Land Model (version 4.5, CLM) to improve simulated forest drought stress and fire, and develop metrics of forest vulnerability to drought based on simulated net primary productivity. Our ultimate objective is to map this vulnerability over the western United States to the middle of this century. Because of uncertainty in human actions to reduce CO₂ emissions, and the need for near-term assessments of carbon consequences of management actions, we focused our analysis on vulnerability during 2020–2049.

2 | MATERIALS AND METHODS

We simulated carbon stocks and fluxes across the western United States (Figure 1) with the Community Land Model (version 4.5, CLM; Oleson et al., 2013). CLM is the land surface component of the community earth system model (Hurrell et al., 2013). We ran CLM at 1/24° × 1/24° (~4-km × 4-km) resolution over the western United States with corresponding climate (details below) and land surface input data (Supporting information Table S1). For efficiency,

calculations were performed only for grid cells with at least 10% forest (79,714 grid cells), as defined by a 250-m resolution forest type map (Ruefenacht et al., 2008).

Community Land Model calculates multiple biophysical and biogeochemical processes, including surface heat fluxes, photosynthesis, evaporation, transpiration, carbon allocation to plant tissue, decomposition, and nitrogen cycling. CLM's default plant functional types (PFTs) represent broad plant categories, such as needle leaf evergreen temperate trees, broadleaf deciduous temperate trees, and C3 grasses. Law et al. (2018) modified CLM physiological parameters to represent major forest types in Oregon to capture species-specific physiological responses to environmental variables. Comparisons with observations showed these modifications greatly improved predictions of biomass within ecoregions. Here, we build upon these modifications to include additional forest types across the western United States (Figure 1).

2.1 | Modifications to the community land model

In addition to having a high spatial resolution (4 km × 4 km), we also enhanced the ecological resolution of CLM by refining the definitions of PFTs. We combined mapped forest types, based on forest inventory data (Ruefenacht et al., 2008), into thirteen PFTs and assigned unique physiological parameters to each (Supporting information Table S2). Because the native resolution of the forest type map is 250 m, our grid cells could have a mixture of up to 13 PFTs. Our number of forest PFTs is limited by the current model structure. Initial physiological parameters for each PFT were selected based on our measured (Berner & Law, 2016) and other published values for the dominant tree species in each PFT. We then varied physiological parameters within the range of observed values and compared simulated aboveground carbon (AGC) with observations over the period 2001–2009 (Wilson, Woodall, & Griffith, 2013) at a subset of 100 grid cells, where each grid cell was composed 100% of a single PFT (1,300 grid cells total), to determine the most appropriate parameter settings (Supporting information Table S2). These calibration simulations were started from equilibrium conditions in 1901 (details below) and run through 2009 to temporally coincide with the gridded AGC estimates in Wilson et al. (2013). The fractional cover of PFTs was normalized to sum to one over the grid cell. We applied the actual percent forest cover in each grid cell (Ruefenacht et al., 2008) in our postprocessing calculations for each output variable of interest. Because we focus on the vulnerability of existing forests, we did not allow forest distributions to change through time by 2049, nor did we model bare ground, shrub, or grass PFTs.

Previous work with CLM in the western United States showed that increased rates of biological nitrogen fixation were required to achieve realistic productivity levels in the coastal forests (Hudiburg, Law, & Thornton, 2013). We applied the same increase in biological nitrogen fixation to forests west of the Cascade Mountains crest.

Community Land Model's relationship between soil moisture and photosynthesis is important for this study's investigation of drought. CLM scales photosynthesis by soil moisture using a factor, β_t , which

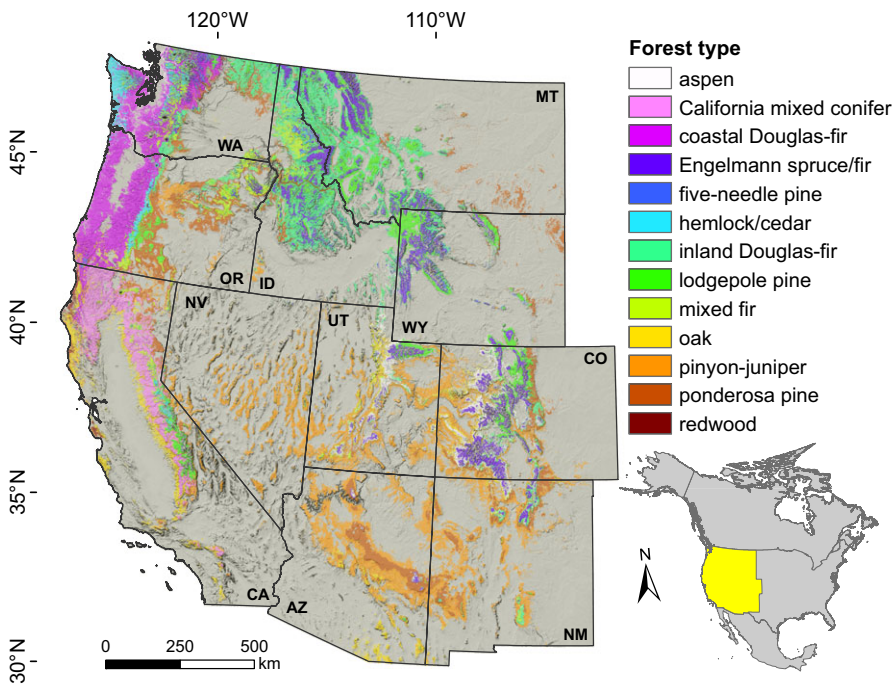


FIGURE 1 Study area showing plant functional types defined in the community land model, shown here at the native 250-m resolution of the forest type map

ranges from one when the soil is saturated to near zero when the soil is completely dry. The maximum potential photosynthesis is scaled by this factor to represent the effects of soil moisture stress (Oleson et al., 2013). In CLM, β_t is calculated using the soil water potential at which stomata close. In this study, we have modified this factor according to species-specific soil water potential values at which half of stem conductivity is lost (Supporting information Table S2), allowing for a reduction in GPP due to drought stress.

Because drought stress can trigger trees to shed leaves (Camarero, Gazol, Sanguesa-Barreda, Oliva, & Vicente-Serrano, 2015), we introduced an algorithm to trigger a reduction in leaf area during periods of drought stress. According to this algorithm, a tree will experience drought stress when the soil moisture drops below the water potential that would cause a 50% decline in hydraulic conductivity (Supporting information Table S2) for a period of 30 consecutive days. Under these conditions, background leaf shed rate (leaf longevity; Supporting information Table S2) increases by 10% until the soil moisture recovers. Leaf shed rate and drought stress duration parameters (Supporting information Figure S1) were selected, based on observations (Kelly, 2016) and comparisons of modeled and plot-level measurements of aboveground carbon in the Sierra Nevada Mountains, CA (Das, Stephenson, & Davis, 2016). Because there are limited empirical data available, we selected parameters that resulted in small increases in leaf shed after severe drought conditions occurred to simulate a conservative response to drought stress.

The CLM fire module was developed to simulate fire at coarser resolutions and across more simply defined vegetation types (Li, Zeng, & Levis, 2012), and modifications were necessary to simulate fire at finer scales. Without modification, area burned was drastically overestimated near urban areas. Therefore, we reduced the effect of

large human populations on fire ignitions. We found that default parameter settings for the upper and lower limits of fuel load that allow fire to spread within a grid cell resulted in repeat burning of some grid cells such that forest regeneration was precluded. This model behavior occurred primarily in lodgepole pine forests in the intermountain states of Wyoming and Colorado, where lodgepole forests currently exist. We also found that fuel loads in our region exceeded the default upper fuel limits, thereby prohibiting fire in some forests in the Pacific Northwest regardless of ignitions. We therefore modified the upper and lower fuel limits on fire spread within grid cells to correspond to the range of forest biomass in our domain.

2.2 | Simulations with the community land model

When first initialized, CLM needs to run long enough for the above and belowground carbon pools to reach a steady state. To accomplish this, we ran CLM for 1,500 model years with bias-corrected 1901–1929 CRUNCEP climate data (Mitchell & Jones, 2005) interpolated from 0.5° resolution to our 1/24° resolution (see Supporting information Appendix S1 for bias correction and interpolation details), using our new forest type parameterizations. We set the fire module to “no fire” and ran for 1,500 model years in accelerated spin-up mode to allow the soil carbon pools to build more quickly (Thornton & Rosenbloom, 2005). We then ran CLM for another 1,000 model years with standard soil carbon accumulation rates and verified that soil and aboveground carbon pools were stable. After carbon stocks reached equilibrium, we ran CLM with bias-corrected CRUNCEP climate data and transient aerosols and CO₂ (Lamarque et al., 2010) from 1901 through 1978 and with our drought and fire modifications active. For the period 1979–2014, we created 3-hourly

climate data by disaggregating (see Supporting information Appendix S2 for details) daily $1/24^\circ \times 1/24^\circ$ (4-km \times 4-km) data (Abatzoglou, 2013). The 1979–2014 climate data served as the reference for the CRUNCEP data bias correction. To account for past disturbance and ensure appropriate spatial representation of stand ages in CLM, we prescribed harvest to achieve stand ages reported for 2008 (Pan et al., 2011). Output from the 1979–2014 simulation was used for model evaluation described below.

A second set of simulations spanning 1979–2049 were run with climate input data from the IPSL-CM5A-MR and MIROC5 general circulation models (GCMs) using historical concentrations (1979–2005) and representative concentration pathway (RCP) 8.5 concentrations (2006–2049) of anthropogenic greenhouse gases (Taylor, Stouffer, & Meehl, 2012) and downscaled as described above. The CLM simulations used the identical concentrations of atmospheric CO₂ as the GCM-derived climate data. We applied harvest during 1979–2008 to achieve 2008 stand age as described above. After 2008, we based harvest amounts on historical harvest data for each state to represent a "business-as-usual" (BAU) scenario (See Supporting information Appendix S3 for details). The 1979–2049 simulations were initialized with output from the simulation using observation-based climate data that ended in 1978 as described above.

We elected to use an RCP 8.5 emissions scenario because it most closely mimics our current emissions (Peters et al., 2013). Moreover, temperature projections under RCPs 4.5 and 8.5 are very similar over the simulation period of 2020–2049 (Supporting information Figure S2), and if there are no vulnerability impacts under an RCP 8.5 scenario, they will not appear under RCP 4.5 (the milder scenario). We selected the IPSL-CM5A-MR and MIROC5 projections because they met the following criteria: (a) The required meteorological variables had been bias-corrected and downscaled to 4-km \times 4-km resolution for the western United States (Abatzoglou, Barbero, Wolf, & Holden, 2014); (b) all required variables were archived for CMIP5 at a 3-hourly interval continuously over the years of interest (Supporting information Table S3); (c) the GCMs sufficiently reproduced a large suite of observed 20th century climate metrics for western North America and the northeast Pacific Ocean—though this is not to say they do not suffer from deficiencies (Rupp, Abatzoglou, Hegewisch, & Mote, 2013). From this set of available GCMs, we selected those that spanned the largest range in temperature and precipitation projected for our region (Supporting information Figure S2a). Across the western United States, the IPSL-CM5A-MR projections are warmer and drier than MIROC5 projections (Supporting information Figure S2b–e). Globally, IPSL-CM5A-MR temperature is approximately one degree higher than MIROC5 temperature by 2050 (Supporting information Figure S3). These two projections span climate conditions that are representative of our current emission trajectory (IPSL-CM5A-MR) and conditions that could be realized if we achieved the globally acknowledged goal of limiting to a 2°C global mean temperature increase (MIROC5).

We also ran a default CLM simulation (no modifications, standard PFTs, $1^\circ \times 1^\circ$ spatial resolution) to determine the magnitude of

differences in simulated carbon stocks and fluxes our model modifications made. This default CLM simulation was "spun-up" as described above and run through 2014 with CRUNCEP climate data and harvest to achieve 2008 stand ages.

2.3 | Model evaluation

First, we quantified over- or underestimation of carbon stocks and fluxes from the modified CLM and the default CLM to determine the level of improvement. Next, we compared our improved CLM-simulated carbon stocks and fluxes with additional inventories and site observations. Where possible, we report the degree of correlation between observations and simulations with linear regression, R^2 , root mean square error (RMSE), and mean bias error (MBE). When observations themselves span a range, we consider model performance to be satisfactory when the simulated estimates fall with the observational range.

We evaluated simulated carbon stocks with gridded aboveground carbon derived from Forest Inventory and Analysis (FIA) plot data (Wilson et al., 2013) across the domain, by state, by PFTs, and by ecoregions (Omernick, 2004). The grid cells that were used in PFT parameter calibration were excluded from this evaluation. We evaluated simulated carbon fluxes with state-level net primary productivity (NPP) derived from MODIS sensors (Berner, Law, & Hudiburg, 2017), FIA-derived carbon fluxes over Oregon, Washington, and California (Hudiburg et al., 2009; Hudiburg, Law, Wirth, & Luysaert, 2011) and observations from five AmeriFlux sites. We evaluated simulated area burned with observed area burned as recorded in the Monitoring Trends in Burn Severity (MTBS) database (Eldenshenk et al., 2007). We compared results of the two drought vulnerability metrics derived from CLM simulations run with observed climate (see below), using published records of forest mortality across the western United States (specific locations and citations in Supporting information Table S9).

2.4 | Vulnerability to drought and fire

Because CLM does not simulate drought-related tree mortality, we developed vulnerability metrics to rank the potential for drought-related mortality based on simulated net primary productivity and tree stem carbon accumulation. Both can decline prior to mortality. There is evidence for the effects of both short-term extreme and prolonged drought on tree mortality (Das, Battles, Stephenson, & Mantgem, 2007; Kane & Kolb, 2014; Macalady & Bugmann, 2014; Sala et al., 2010), and we defined metrics to represent vulnerability to either of these conditions.

We defined short-term drought as the conditions that could lead to tree mortality in one year. We used a metric common to many dynamic vegetation models, in which 100% mortality occurs when annual NPP = 0 (Krinner et al., 2005; Levis, Bonan, Vertenstein, & Oleson, 2004; Sitch et al., 2003). For each decade (2020–2029, 2030–2039, 2040–2049), we defined low short-term drought vulnerability as 0 years with NPP = 0; medium short-term drought

vulnerability as 1 year with NPP = 0; and high short-term drought vulnerability as 2+ years with NPP = 0.

We defined vulnerability to prolonged drought as a function of allocation to growth. Allocation to growth is a low priority for mature trees (Waring, 1987), and the probability of mortality increases as the number of years of no growth increases (Allen & Breshears, 1998; Kane & Kolb, 2014; Wyckoff & Clark, 2002). Based on the number of observed years with no growth and subsequent mortality reported in these field studies, for each decade, we defined low vulnerability to prolonged drought as 0 years with low allocation to growth; medium vulnerability to prolonged drought as 1–3 years with low allocation to growth; and high vulnerability to prolonged drought as 4+ years with low allocation to growth. We defined low allocation as stem allocation <0.1% of aboveground carbon based on field observations (Baldocchi et al., 2010; Law, Thornton, Irvine, Anthoni, & Tuyl, 2001).

Final drought vulnerability per decade was calculated as the maximum of either short-term or prolonged drought during each decade for each grid cell, for each climate projection. We explicitly incorporated uncertainty due to future climate projections into our vulnerability metrics by defining final drought vulnerability classes where:

1. Uncertain = one GCM low and one high
2. Low = both GCMs low
3. Med-Low = one low and one medium
4. Medium = both GCMs medium
5. Med-High = one medium and one high
6. High = both GCMs high

We represented future vulnerability to fire based on the difference in simulated future (2020–2049) minus simulated past (1980–2009) area burned weighted by the future area burned. We normalized future area burned by the maximum area burned in any grid cell, from either climate-forcing simulation (IPSL-CM5A-MR or MIROC5). We then weighted the difference in future minus past by the normalized future area burned. The resulting distribution of weighted differences in area burned was classified into low, medium, and high fire vulnerability by terciles. Final fire vulnerability rankings accounted for differences due to climate projections, as did final drought vulnerability.

Because there were differences between the simulated and observed area burned (see Results), we assessed the influence of this uncertainty in simulated area burned on our vulnerability classifications. We calculated the ratio of CLM-predicted versus observed area burned during 1984–2012 at the spatial resolution of ecoregions (see Supporting information Figure S5e) and multiplied the area burned over 1979–2049 for each grid cell by this ratio. We then calculated fire vulnerability from these adjusted area burned values and compared with the unadjusted vulnerability rankings to identify where uncertainty in CLM-simulated burn area may lead to uncertainty in future fire vulnerability.

We determined combined drought and fire vulnerability in two ways, (a) the maximum of *either* drought or fire and (b) the

combination of *both* drought and fire. For the second method, we identified six vulnerability classes using the method described above for combining results from the two climate projections.

We examined characteristics of grid cells that experienced decreasing, constant, and increasing vulnerability to drought over time by calculating the change in temperature, precipitation, soil moisture stress (CLM transpiration beta factor), and carbon stocks between decades. Since fire vulnerability was based on the differences between the past and future period, we assessed the above characteristics in low, medium, and high vulnerability classes over the future period 2020–2049.

3 | RESULTS

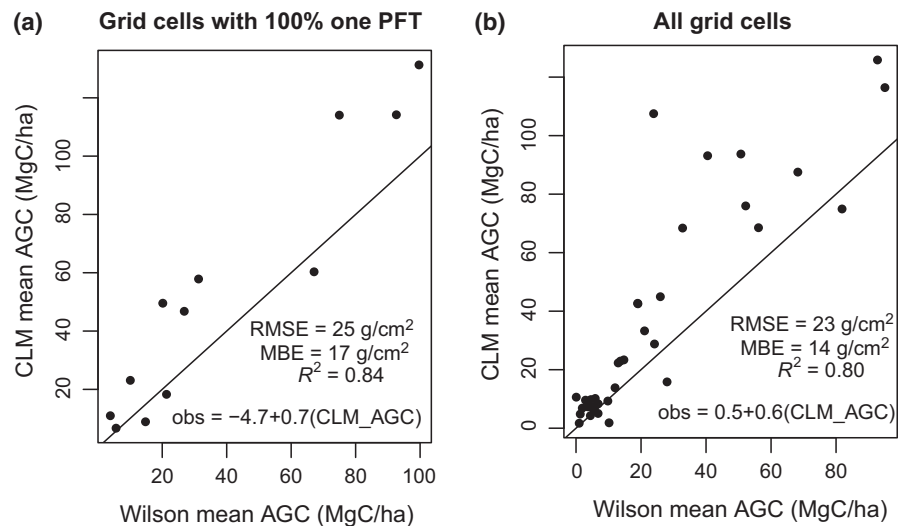
3.1 | Model evaluation

Our modifications strongly improved CLM's performance in forested areas of the western United States. Using CLM with no modifications, total domain-wide aboveground live-tree carbon (AGC) in forests was underestimated by a factor of 11 compared with observation-based AGC estimates during 2001–2009, and total simulated annual area of forest burned was overestimated by a factor of 20 during 1984–2012 (Supporting information Figure S4). With our modifications, both aboveground carbon and area burned were overestimated by a factor of 2.

Our modifications produced satisfactory simulations of carbon stocks and fluxes over the western United States. Simulated AGC was highly correlated with observation-based AGC when evaluated across forest types ($R^2 = 0.84$, Figure 2a) and across ecoregions ($R^2 = 0.80$, Figure 2b). Across the region, simulated mean aboveground carbon (AGC) was within one standard deviation of observed AGC (Obs. mean = 30.5 Mg C/ha, SD = 39.7 Mg C/ha, CLM mean = 59.1 Mg C/ha, SD = 45.5 Mg C/ha). Comparisons of observed and simulated AGC for those grid cells with 100% single PFT composition, (Figure 2a), indicated the physiological parameterizations for each PFT were appropriate. Simulated mean AGC for 12 of 13 PFTs was within one standard deviation of the observed mean, and the lodgepole pine mean was within two standard deviations (Supporting information Figure S5). CLM tended to overestimate AGC more in the intermountain regions than in the coastal regions (Supporting information Figure S5).

The modified CLM satisfactorily simulated NPP. Domain- and state-wide CLM estimates of NPP fell within the range of NPP estimates derived from MODIS and FIA data (Supporting information Table S4) and were highly correlated with mean state-level MODIS NPP estimates ($R^2 = 0.98$, RMSE = 16 Mg C/ha, MBE = -3 Mg C/ha). Comparison with FIA data from Oregon indicates CLM overestimated net primary productivity (NPP) by 6.9% and heterotrophic respiration by 15.1% and underestimated net ecosystem productivity by 4.2% (Supporting information Table S5). Patterns of carbon flux over- and underestimation varied by ecoregion within Oregon (Supporting information Table S5). For 34 forested plots in Oregon and California that were within 13 CLM grid cells, CLM tended to

FIGURE 2 Comparison of aboveground carbon between observation-based gridded estimates (Wilson) and CLM-simulated estimates averaged over (a) plant functional type (forest type, $n = 13$) and (b) ecoregion ($n = 13$), showing root mean square error (RMSE), mean bias error (MBE), R^2 , linear regression equation, and 1:1 line



overestimate NPP and heterotrophic respiration, leading to an average 7% overestimation of annual NEP (Supporting information Figure S6). Across four coniferous forest AmeriFlux sites, CLM underestimated gross primary productivity (GPP) by 6.8% (Supporting information Table S6), overestimated ecosystem respiration by 10.6% (Supporting information Table S7), and overestimated net ecosystem productivity by 0.6% (Supporting information Table S8). At an oak woodland AmeriFlux site (Ma, Baldocchi, Xu, & Hehn, 2007), CLM underestimated NPP by 12.3%.

Over the western United States, our modified CLM estimates of area burned were highly correlated with observations ($R^2 = 0.75$, Figure 3). CLM overestimated the total forested area burned during 1984–2012 by 28.6% relative to burn area reported in the MTBS data (Eldenshenk et al., 2007; Supporting information Figure S7). CLM tended to overestimate area burned in the lowest and highest carbon-density forests (Supporting information Figure S7). However, Whittier and Gray (2016) determined that MTBS underestimates burn area by 20% when compared with inventory data, which implies CLM overestimates may be as low as 8%. We consider these metrics to indicate satisfactory model performance. We address the potential consequences of uncertainty in simulated area burned below.

Observed plot-level tree mortality corresponded well with our drought mortality metrics. Twelve of thirteen sites with observed mortality between 1989 and 2009 had at least one year with no allocation to growth or zero NPP in the preceding 5 years, resulting in medium to high vulnerability classification (Supporting information Table S9). Of the six sites with observed mortality rates higher than 50%, four were classified with high drought vulnerability, one with medium, and one with low. Widespread pinyon pine mortality was observed in Arizona and New Mexico in 2003 and 2004 (Breshears et al., 2005), and CLM simulations showed widespread occurrence of years with no allocation to growth and $NPP = 0$ (medium to high vulnerability) during 1997–2003 (Supporting information Figure S8). Areas with multiple years with no allocation to growth and with $NPP = 0$ (medium to high vulnerability) also coincide with observed

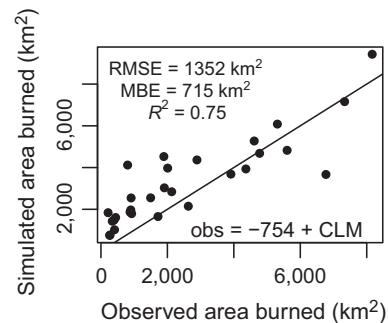


FIGURE 3 Comparison of observed (MTBS) and CLM-simulated area burned each decade, showing root mean square error (RMSE), mean bias error (MBE), R^2 , linear regression equation, and 1:1 line

bark beetle mortality during 1997–2010 (Supporting information Figure S8). Although we are not able to perform a test for omission, these comparisons do not show high historical drought vulnerability in regions without recorded tree mortality.

3.2 | Historical simulations with GCM climate projections

Compared to CLM simulations run with observed climate, CLM simulations using IPSL-CM5A-MR and MIROC5 climate projections over 1979–2014 resulted in similar values for AGC and similar number of years with no allocation to growth and with $NPP = 0$ (Supporting information Figure S9). Area burned under GCM projections did not increase as quickly as area burned using observed climate (Figure 4) and was approximately 22% lower in the 2010s. We address this source of uncertainty in our future estimates of fire vulnerability as described below.

The IPSL-CM5A-MR climate projections tend to be drier and warmer than the MIROC5 projections (Supporting information Figure S10). Averaged over the domain, IPSL-CM5A-MR projections are 3.5° warmer in the 2040s than the 1980s, and MIROC5 projections are 3.1° warmer. Neither projection shows substantial changes

in precipitation between time periods when averaged across the domain (Supporting information Figure S10).

3.3 | Future forest vulnerability to drought

Future forest vulnerability to prolonged drought (Supporting information Figure S11) is expected to be more widespread than vulnerability to short-term drought (Supporting information Figure S12). Future estimates of prolonged drought differ less between climate projections than do estimates of short-term drought vulnerability. Combined drought vulnerability (Supporting information Figure S13), described below, is the maximum of prolonged or short-term drought vulnerability.

Forest vulnerability to drought stress between 2020 and 2049 varies widely across the western United States (Figure 5a). Low drought vulnerability, covering 64% of the domain (Table 1), is expected across most of the coastal and western Cascade regions and portions of northern Idaho and Montana. Widespread areas of low to medium drought vulnerability are expected throughout the intermountain west, covering about 9% of the forest area. Large portions of the southern Rocky Mountains in Wyoming, Colorado, Utah, Arizona, and New Mexico, covering 36% of the domain, are expected to experience medium to high vulnerability to drought regardless of climate projection (Figure 5a). Scattered pockets of medium to high drought vulnerability are also expected throughout the Sierra Nevada, northern Rocky Mountains, and eastern Oregon. Importantly, differences between the climate projections do not result in conflicting low and high drought vulnerability classifications in near-future decades and very little area with medium–low and medium–high vulnerability rankings. Where drought vulnerability predictions differed between climate projections, the warmer IPSL-CM5A-MR projections resulted in higher vulnerability (not shown).

Thus, areas with medium–low and medium–high vulnerability (Table 1) indicate the differences in future drought vulnerability under a current trajectory emission scenario (represented by the IPSL-CM5A-MR climate projections) and a limited warming scenario (represented by MIROC5 climate projections). Limited warming would reduce drought vulnerability in 13% of the forested western United States compared with a current trajectory scenario (Table 1). Across the western United States, the potential for future forest mortality from drought, as indicated by the area of forest in each vulnerability category, is expected to remain similar to the past few decades (Supporting information Figure S14).

From one decade to the next, drought vulnerability tended to increase at the edges of forest type distributions. Grid cells at distribution edges necessarily had a low percent cover of a given forest type, and these were the grid cells that experienced an increase in drought vulnerability (Supporting information Figure S15a). As expected, drought vulnerability also increased where, from one decade to the next, soil moisture was more limiting as represented by the change in the soil transpiration factor (Supporting information Figure S16b), annual precipitation was lower (Supporting information Figure S16c), and annual temperature was higher (Supporting information Figure S16d). Changes in drought vulnerability did not appear to be correlated with changes in AGC (Supporting information Figure S16a).

The pinyon-juniper forest type is expected to be the most vulnerable to drought, with only about 20% of its range expected to have low vulnerability (Supporting information Figure S17). Most forest types are expected to experience high drought vulnerability in some portion of their ranges. However, coastal Douglas-fir, hemlock/cedar, and redwood forest types are expected to experience only low drought vulnerability by mid-21st century (Supporting information Figure S17). Relative vulnerability rankings across forest types (Supporting information Figure S17) remain mostly consistent from the 1990s through the 2040s (not shown).

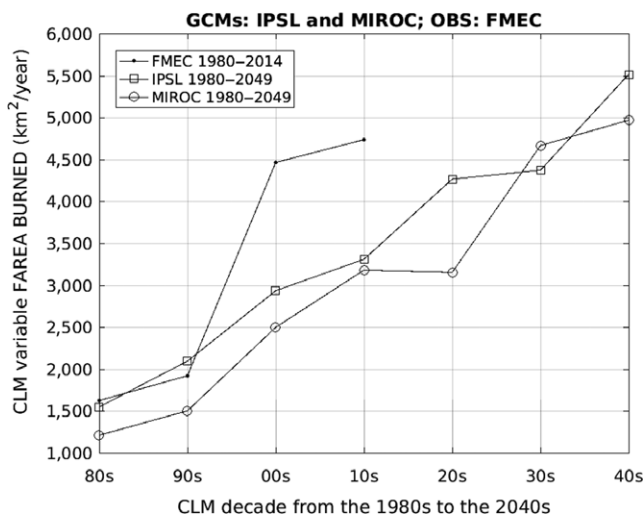


FIGURE 4 Area burned from CLM simulations run with observation-based climate (FMEC) and projections from two general circulations models (IPSL-CM5A-MR and MIROC5) under RCP8.5

3.4 | Future forest vulnerability to fire

Future area burned is expected to increase under both climate projections (Figure 4), primarily in the Sierra Nevada and Rocky Mountains (Supporting information Figure S18). Between 2020 and 2049, most (82%) of the western United States is predicted to experience low vulnerability to fire regardless of climate projections (Table 1, Figure 5b). High fire vulnerability, covering 14% of the domain, is primarily expected in the intermountain region, the Sierra Nevada, and Klamath Mountains. Differences between climate projections lead to only 1% of the forested domain with conflicting low and high fire vulnerability (Figure 5b). A limited warming scenario reduces fire vulnerability in 5% of the forested domain compared with a current trajectory scenario (Table 1). After incorporating uncertainty due to differences between observed and simulated area burned, fire vulnerability over 87% of the domain remained unchanged, approximately 3% increased (mostly in CA and southern OR), 3% decreased (mostly in the Rocky Mountains), and 7% switched to uncertain fire

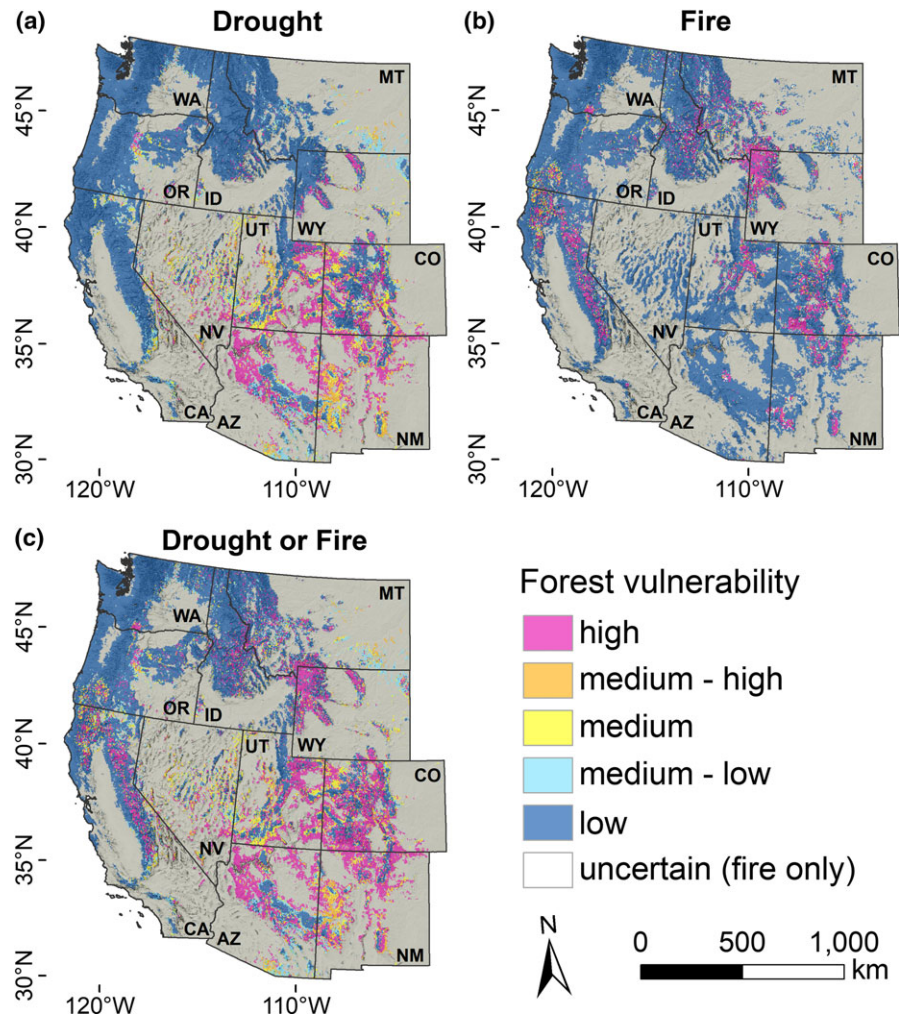


FIGURE 5 Vulnerability of forested areas during 2020–2049 to (a) drought, (b) fire, and (c) either drought or fire. Colors indicate agreement between CLM simulations with two climate projections, where one GCM low and one high (uncertain) = gray, both GCMs low = dark blue, one low one med = cyan, both medium = yellow, one medium one high = orange, and both high = magenta

TABLE 1 Forested area (km²) in each drought, fire, and total (maximum of drought or fire) vulnerability category during 2020–2049

	Uncertain	Low	Medium–Low	Medium	Medium–High	High
Drought	0	815,600	108,960	86,960	63,248	201,936
Fire	13,728	1,046,160	33,840	17,680	25,520	139,776
Total	0	651,616	118,544	93,952	75,184	337,408

Note. Categories reflect agreement between CLM simulations run with two climate projections, as described in the main text.

vulnerability (mostly in the CO Rocky Mountains and eastern WA; Supporting information Figure S19).

Fire vulnerability tended to be highest where average decadal precipitation during 2020–2049 increases was the smallest (Supporting information Figure S20). In general, grid cells that accumulated AGC were in more mesic ecoregions and experienced low fire vulnerability. Relationships between fire vulnerability and changes in soil moisture stress or temperature were not apparent (Supporting information Figure S20).

Redwood is the only forest type expected to experience only low vulnerability to fire (Supporting information Figure S21). The expected area with high fire vulnerability is primarily composed of inland Douglas-fir, lodgepole pine, ponderosa pine, CA mixed conifer,

and mixed fir forest types, representing approximately 10%–20% of each forest type's range (Supporting information Figure S21).

3.5 | Future forest vulnerability to fire and drought

Differences in the spatial distribution of drought and fire vulnerability lead to 40% of the forested areas in the western United States expected to experience medium to high vulnerability to drought or fire at some time during 2020 through 2049 (Figure 5c). Pinyon-juniper is the most vulnerable forest type, with more than 40% of its range expected to experience high vulnerability to drought or fire, regardless of climate projections (Figure 6). Just over half of the forested area, primarily in the coastal regions, is expected to have

low vulnerability to drought or fire (Figure 5c). The coastal Douglas-fir, hemlock/cedar, and redwood forest types are expected to experience low vulnerability to drought or fire (Figure 6). All other forest types are expected to experience high vulnerability to drought or fire in at least 10% of their range, regardless of climate projections (Figure 6).

Approximately 2% of the forested western United States is expected to experience medium-high or high vulnerability to both drought and fire (Supporting information Figure S22). The majority of this high vulnerability area is composed of pinyon-juniper, oak, and ponderosa pine forest types, and represents less than 5% of those PFTs ranges (Supporting information Figure S23).

4 | DISCUSSION

Our modifications to CLM were essential for characterizing forest ecosystem processes with increased ecological resolution and estimating forest vulnerability to drought and fire. Comparisons with

historical observations indicate that the physiological parameterizations we developed for specific forest types produced accurate simulations of historical carbon stocks and fluxes, with both observation-based and GCM-hindcast climate data. This increases our confidence in our simulated near-future carbon stocks and fluxes.

Here, drought stress triggered leaf shed, which limited photosynthetic capacity. Our drought vulnerability metrics showed medium to high vulnerability in places that recently experienced drought-related mortality, and vulnerability increased where soil moisture, temperature, and precipitation indicated drought conditions existed. These metrics are therefore likely to identify areas that may experience tree mortality due to drought stress in the near future.

Insects contributed to mortality in many of the documented instances of recent drought-related mortality in the western United States (Allen et al., 2010; Anderegg et al., 2015). Our estimated drought vulnerability during 1996–2010 corresponded with areas of beetle mortality in the Rocky Mountains and Southwest United States (Berner, Law, Meddens, & Hicke, 2017; Meddens, Hicke, &

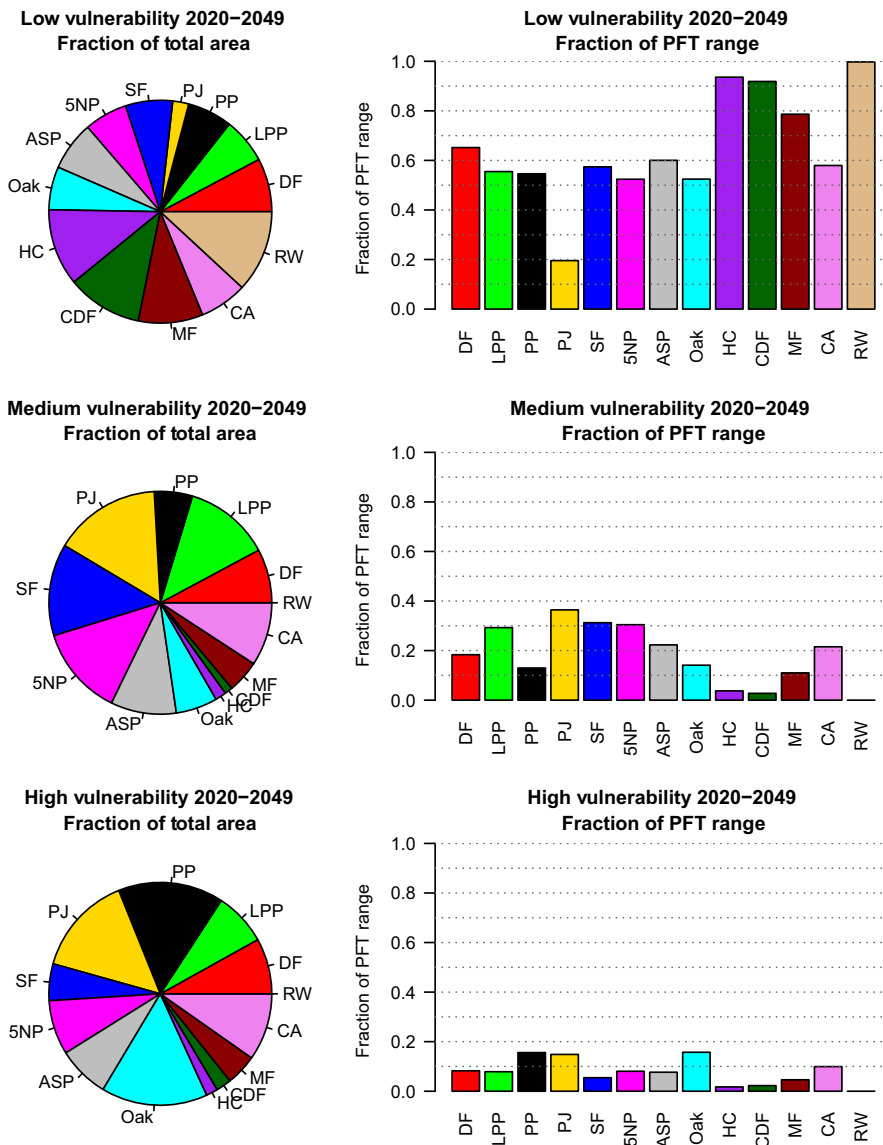


FIGURE 6 Composition of PFTs (pie charts) and percent of each PFT range (bar charts) where either drought or fire vulnerability is low, medium, and high

Ferguson, 2012); however, we do not account for direct effects of climate on beetle development and survival (Bentz et al., 2010) that can lead to beetle population increases. Therefore, our metrics may identify forested areas vulnerable to beetle attack due to the presence of drought-stressed trees (Boone, Aukema, Bohlmann, Carroll, & Raffa, 2011; Breshears et al., 2005), but do not necessarily represent forest vulnerability to aggressive bark beetle outbreaks in which healthy trees may be killed (Raffa et al., 2008). Consequently, we do not include an interaction between insect outbreaks and fire. This is unlikely to have a strong impact on estimated fire vulnerability because wildlife likelihood does not consistently increase or decrease following insect outbreaks (Hicke, Johnson, Jane, & Preisler, 2012; Meigs et al., 2015).

Several studies have indicated that future forest mortality in the western United States is likely to increase due to drought stress (Allen et al., 2010; Jiang et al., 2013; Thorne et al., 2018; Williams et al., 2013). Our analyses indicate strong potential for continued levels of drought-related forest mortality in the Southern Rocky Mountains and southwestern regions of the United States in the coming decades under both climate projections. Recent estimates of climate change vulnerability across the southwestern United States identified similar regions with high exposure to climate change (Thorne et al., 2018). Together, this evidence suggests that forests in the Southwest are likely to suffer from a changing climate. We show a relatively constant area with high drought vulnerability through time, which may be related to our categorical, instead of continuous, drought vulnerability metric. Given the current lack of understanding of direct mechanisms controlling tree mortality (McDowell et al., 2008; Sala et al., 2010), we elected to use a categorical vulnerability metric, based on observations of mortality under specific growth and productivity conditions.

We expect Pinyon-juniper, the most common forest type in the Southwest, to be the most vulnerable to drought-related mortality in the near future. Pinyon-juniper shows simulated vulnerability to both short-term and prolonged drought, as has been documented in field studies (Macalady & Bugmann, 2014). Observations indicate recent drought-related mortality has affected pinyon pine more than juniper (Breshears et al., 2005). Our physiological parameterizations for the pinyon-juniper forest reflect pinyon hydrologic traits. Juniper components of these forests may therefore be less vulnerable to future drought-related mortality than our metrics indicate.

Previous studies have indicated a high level of climate change exposure in the foothills of CA (Thorne et al., 2017, 2018). We do not identify high drought vulnerability in this area, which can indicate that either those forest types (primarily oak and CA mixed conifer) are able to withstand a large deviation from their historical climate conditions or that we have underestimated the influence of drought on their physiology. Further field and modeling experiments could help clarify forest sensitivity to drought in this region.

We identify low drought vulnerability across large areas of the Pacific Northwest and Northern Rocky Mountains. Simulations with a dynamic vegetation model show expanding forest area in these regions at the end of this century (Shafer, Bartlein, Gray, & Peltier,

2015). Other dynamic vegetation model simulations indicate contracting needle leaf evergreen forest cover in some areas we identify as having low drought vulnerability (Jiang et al., 2013). Given the improvements our modifications made compared with standard CLM evergreen needle leaf forest parameterizations, these differences may well be due to species-level physiological sensitivity to climate extremes.

Anthropogenic climate change is a contributing factor in recent increases in area burned in the western United States (Abatzoglou & Williams, 2016), and future climate is expected to exert a strong influence on fire occurrence (Pechony & Shindell, 2010). Our fire vulnerability metric identified regions with high expected future burned area as well as areas with large increases in area burned relative to the recent past. The central and southern Rocky Mountains, where fire is most common, are expected to experience high vulnerability to fire in both absolute and relative area burned. Other areas with high future fire vulnerability occur throughout the northern Rocky Mountains, the East Cascades, and Sierra Nevada. Broadly, the spatial distribution of increases in area burned and fire vulnerability shown here agrees with results from several studies that took a statistical approach to simulating future fire (Kitzberger, Falk, Westerling, & Swetnam, 2017; Moritz et al., 2012). Our estimates of high fire vulnerability also agree with projections of more frequent fire in the Greater Yellowstone Ecosystem (Westerling, Turner, EaH, Romme, & Ryan, 2011) and increasing area burned in the Klamath and Sierra Mountains of CA (Westerling, Hidalgo, Cayan, & Swetnam, 2006). Notable areas with large projected increases in fire in CA (Westerling et al., 2006) along the CA coast are in shrub types, which we did not assess. Shortening of the historical fire return interval has the potential to trigger a vegetation shift (Westerling et al., 2011) in any of these regions.

Areas identified as highly vulnerable to fire are expected to be more likely to burn in the near future than in the historical period. With this statement, we do not imply that areas labeled highly vulnerable *will* burn or that if ignited they will burn with high intensity. Simulated fire ignition outside of urban areas depends on lightning strikes. Because lightning is difficult to predict, we rely on observations of historical lightning strikes to estimate future ignitions. Severity is a measure of the effect of fire intensity on the ecosystem and is determined by fire weather, fuel conditions, terrain, and vegetation type (Parks et al., 2018). Most contemporary fires in mixed conifer forests of western North America are mixed-severity fires. In the Pacific Northwest, mixed-severity fires include unburned and low severity areas that account for 50%–60% of total burn area, and only 13% of total burn area experiences high severity (90% tree mortality; Halofsky et al., 2011; Law & Waring, 2015). The current CLM fire module does not estimate fire severity. Thus, a classification here of highly vulnerable to fire does not imply those areas will experience high severity fire. Finally, human efforts to suppress fires have a strong influence of area burned, and the CLM fire module does not account for fire suppression policies.

We expect total vulnerability, to *either* drought or fire, to be lowest in Coastal Douglas-fir, hemlock/cedar, and redwood forest types.

Because of their high carbon-density, longevity, mesic growing conditions, and relatively long fire return intervals, these forests have the greatest potential to sequester carbon of any forests in the western United States (Law et al., 2018). Therefore, regional policies that promote forest stewardship as a natural solution to climate change mitigation (Griscom et al., 2017) should be investigated.

Widespread vulnerability to drought or fire, and therefore elevated risk of forest mortality, is expected in the Rocky Mountains, Sierra Nevada, Southwest, and Great Basin regions of the western United States. Because mortality has the potential to lead to changes in forest composition and transitions to non-forest vegetation types (Allen & Breshears, 1998; Anderegg, Kane, & Anderegg, 2012; Veblen, Hadley, Reid, & Rebertus, 1991; Williams et al., 2013), our vulnerability estimates indicate these regions have the potential to experience substantial ecological change in the coming decades. In these regions, research on the effects of land management practices, for example, thinning effects on surface temperature, canopy heating, and seedling establishment (von Arx, Pannatier, Thimonier, & Rebetez, 2013), on future drought and fire vulnerability and regional carbon balance, could inform and guide land management policies.

We expect the greatest potential for ecological change to be concentrated in Pinyon-juniper, oak, and ponderosa pine forests across the southern Rocky Mountains and Southwest United States, where future vulnerability to *both* fire and drought is high. Forests in these areas are primarily water limited (Nemani et al., 2003), and mortality in these forests is of particular concern. Mortality can increase the amount of forest edge, and productivity tends to decrease along forest edges in water-limited systems due to increased drought stress (Smith, Hutrya, Reinmann, Marrs, & Thompson, 2018). Additionally, we found increasing vulnerability in mixed forests (low percent cover of any given forest type), indicating mortality may be the highest at the margins of forest type distributions and within ecotones (Neilson, 1993). Future climate conditions may preclude reestablishment of existing species, thereby accelerating shifts in forest distributions (Allen & Breshears, 1998). Additional field research and model development to guide-assisted migration policies (Neilson et al., 2005) may be most relevant in this region.

We selected two GCM projections that cover a medium to high regional response to greenhouse gas forcing. Even so, there was very little variation in carbon stocks and fluxes between climate simulations, and no portion of the western United States was classified with conflicting low and high drought vulnerability. This agreement is likely due in part to variability at multiple temporal scales, whereby the definitions of high vulnerability are exceeded in each climate simulation at different times but still occurs during a decade.

Mortality events and vegetation state shifts can have long-term effects on carbon cycling and sequestration potential (Hudiburg, Higuera, & Hicke, 2017; McLauchlan et al., 2014) and important feedbacks to climate (Anderegg, Kane, et al., 2012; Bonan, 2008). Therefore, simulating forest mortality is a critical component of earth system models (Bonan & Doney, 2018). Our work is a step toward incorporating more refined plant strategies and drought-related mortality in an earth system model (van der Molen et al., 2011). We

demonstrate that physiological representation of multiple forest types is critical for reliable simulations of historical carbon stocks and fluxes in the western United States (Duarte et al., 2016; Hudiburg et al., 2013). An assessment of available physiological data and model sensitivity tests are necessary to determine which forest type distinctions are achievable and most important at the global scale. Given the uncertainty in the direct mechanisms of tree mortality due to drought (McDowell et al., 2011, 2008; Sala et al., 2010), identifying the conditions under which trees are likely to succumb to drought-related mortality may be a viable alternative to implementing physiological mortality mechanisms in ESMs (Anderegg, Berry, et al., 2012). Our drought mortality metrics could be implemented as mortality algorithms by defining forest type-specific probability of mortality when the metric conditions are met (Hartmann et al., 2018). A logical extension is to implement such algorithms in a dynamic vegetation model, thereby allowing for the potential for drought-induced mortality to cause vegetation state shifts, which in turn can influence fire occurrence and spread.

Under future climate conditions represented by two general circulation models and the highest CO₂ scenario (RCP8.5), forest vulnerability to drought-related and fire mortality is likely to continue at recent levels or increase in the near future, depending on location and environmental conditions. Forests in the Southwest are the most vulnerable and therefore have the greatest risk of conversion to a different vegetation type in the near future. Forests in the Pacific Northwest are least likely to experience future drought and fire mortality. Our work demonstrates that increased physiological detail and new drought stress algorithms in land surface models are critical for simulating future forest mortality. These modifications have the potential to be implemented in other near-future regional assessments. Implementation in a coupled land-atmosphere earth system model will have the added benefit of representing forest mortality and vegetation state shifts and their feedbacks to climate. These abilities are essential for evaluating land management strategies and energy policies.

ACKNOWLEDGMENTS

We thank Dr. Jeffrey Hicke and Dr. David Lawrence for support in working with CLM, Dr. Logan Berner for creating Figures 1 and 5, and two anonymous reviewers for comments that distinctly improved the manuscript. This research was supported by the Agriculture and Food Research Initiative of the US Department of Agriculture National Institute of Food and Agriculture (Grants 2013-67003-20652, 2014-67003-22065, and 2014-35100-22066) for our North American Carbon Program studies, "Carbon cycle dynamics within Oregon's urban-suburban-forested-agricultural landscapes," and "Forest die-off, climate change, and human intervention in western North America," and the Office of Science (BER), US Department of Energy (DOE Grant No. DE-FG02-07ER64361). We thank the AmeriFlux network and Dr. Hyojung Kwon for processing the flux site data for evaluating CLM performance. High-performance computing resources on Cheyenne (<https://doi.org/10.5065/D6RX99HX>)

were provided by NCAR's Computational and Information Systems Laboratory, sponsored by the National Science Foundation.

ORCID

Polly C. Buotte  <http://orcid.org/0000-0002-6572-2878>

Beverly E. Law  <http://orcid.org/0000-0002-1605-1203>

REFERENCES

- Abatzoglou, J. T. (2013). Development of gridded surface meteorological data for ecological applications and modelling. *International Journal of Climatology*, 33, 121–131. <https://doi.org/10.1002/joc.3413>
- Abatzoglou, J. T., Barbero, R., Wolf, J. W., & Holden, Z. A. (2014). Tracking interannual streamflow variability with drought indices in the U.S. Pacific Northwest. *Journal of Hydrometeorology*, 15, 1900–1912. <https://doi.org/10.1175/JHM-D-13-0167.1>
- Abatzoglou, J. T., & Williams, A. P. (2016). Impact of anthropogenic climate change on wildfire across western US forests. *Proceedings of the National Academy of Sciences of the United States of America*, 113, 11770–11775. <https://doi.org/10.1073/pnas.1607171113>
- Allen, C. D., & Breshears, D. D. (1998). Drought-induced shift of a forest/woodland ecotone: Rapid landscape response to climate variation. *Proceedings of the National Academy of Sciences of the United States of America*, 95, 14839–14842. <https://doi.org/10.1073/pnas.95.25.14839>
- Allen, C. D., Macalady, A. K., Chenchouni, H., Bachelet, D., McDowell, N., Vennetier, M., ... Cobb, N. (2010). A global overview of drought and heat-induced tree mortality reveals emerging climate change risks for forests. *Forest Ecology and Management*, 259, 660–684. <https://doi.org/10.1016/j.foreco.2009.09.001>
- Anderegg, W. R. L., Berry, J. A., & Field, C. B. (2012). Linking definitions, mechanisms, and modeling of drought-induced tree death. *Trends in Plant Science*, 17, 693–700.
- Anderegg, W. R., Hicke, J. A., Fisher, R. A., Allen, C. D., Aukema, J., Bentz, B., ... Pan, Y. (2015). Tree mortality from drought, insects, and their interactions in a changing climate. *New Phytologist*, 208, 674–683. <https://doi.org/10.1111/nph.13477>
- Anderegg, W. R. L., Kane, J. M., & Anderegg, L. D. L. (2012). Consequences of widespread tree mortality triggered by drought and temperature stress. *Nature Climate Change*, 3, 30–36.
- Anderegg, W. R. L., Klein, T., Bartlett, M., Sack, L., Pellegrini, A. F. A., Choat, B., & Jansen, S. (2016). Meta-analysis reveals that hydraulic traits explain cross-species patterns of drought-induced tree mortality across the globe. *Proceedings of the National Academy of Sciences of the United States of America*, 113, 5024–5029. <https://doi.org/10.1073/pnas.1525678113>
- Baldocchi, D., Chen, Q., Chen, X., Ma, S., Miller, G., Ryu, Y., ... Battles, J. (2010). The dynamics of energy, water and carbon fluxes in a Blue Oak (*Quercus douglasii*) Savanna in California, USA. *Ecosystem Function in Savannas, 2010*, 135–154.
- Bentz, B. J., Régnière, J., Fettig, C. J., Hansen, E. M., Hayes, J. L., Hicke, J. A., ... Seybold, S. J. (2010). Climate change and bark beetles of the western United States and Canada: Direct and indirect effects. *BioScience*, 60, 602–613. <https://doi.org/10.1525/bio.2010.60.8.6>
- Berner, L. T., & Law, B. E. (2016). Plant traits, productivity, biomass and soil properties from forest sites in the Pacific Northwest, 1999–2014. *Nature Scientific Data*, 3, 1999–2014. <https://doi.org/10.1038/sdata.2016.2>
- Berner, L. T., Law, B. E., & Hudiburg, T. W. (2017). Water availability limits tree productivity, carbon stocks, and carbon residence time in mature forests across the western US. *Biogeosciences*, 14, 365–378.
- Berner, L. T., Law, B. E., Meddens, A. J. H., & Hicke, J. A. (2017). Tree mortality from fires, bark beetles, and timber harvest during a hot and dry decade in the western United States (2003–2012). *Environmental Research Letters*, 12(6):065005.
- Bonan, G. B. (2008). Forests and climate change: Forcings, feedbacks, and the climate benefits of forests. *Science*, 320, 1444–1449. <https://doi.org/10.1126/science.1155121>
- Bonan, G. B., & Doney, S. C. (2018). Climate, ecosystems, and planetary futures: The challenge to predict life in Earth system models. *Science*, 359, eaam8328.
- Boone, C. K., Aukema, B. H., Bohlmann, J., Carroll, A. L., & Raffa, K. F. (2011). Efficacy of tree defense physiology varies with bark beetle population density: A basis for positive feedback in eruptive species. *Canadian Journal of Forest Research*, 41, 1174–1188. <https://doi.org/10.1139/x11-041>
- Breshears, D. D., Cobb, N. S., Rich, P. M., Price, K. P., Allen, C. D., Balice, R. G., ... Anderson, J. J. (2005). Regional vegetation die-off in response to global-change-type drought. *Proceedings of the National Academy of Sciences of the United States of America*, 102, 15144–15148. <https://doi.org/10.1073/pnas.0505734102>
- Camarero, J. J., Gazol, A., Sanguesa-Barreda, G., Oliva, J., & Vicente-Serrano, S. M. (2015). To die or not to die: Early warnings of tree die-back in response to a severe drought. *Journal of Ecology*, 103, 44–57. <https://doi.org/10.1111/1365-2745.12295>
- Das, A. J., Battles, J. J., Stephenson, N. L., & Van Mantgem, P. J. (2007). The relationship between tree growth patterns and likelihood of mortality: A study of two tree species in the Sierra Nevada. *Canadian Journal of Forest Research-Revue Canadienne De Recherche Forestiere*, 37, 580–597. <https://doi.org/10.1139/X06-262>
- Das, A. J., Stephenson, N. L., & Davis, K. P. (2016). Why do trees die? Characterizing the drivers of background tree mortality. *Ecology*, 97, 2616–2627. <https://doi.org/10.1002/ecy.1497>
- Duarte, H. F., Raczka, B. M., Ricciuto, D. M., Lin, J. C., Koven, C. D., Thornton, P. E., ... Ehleringer, J. R. (2016). Evaluating the community land model (CLM 4.5) at a coniferous forest site in Northwestern United States using flux and carbon-isotope measurements. *Biogeosciences Discuss* 14(18): 4315–4340.
- Eldenshenk, J., Schwind, B., Brewer, K., Zhu, Z., Quayle, B., & Howard, S. (2007). A project for monitoring trends in burn severity. *Fire Ecology Special Issue*, 3(1), 3–21.
- Griscom, B. W., Adams, J., Ellis, P. W., Houghton, R. A., Lomax, G., Miteva, D. A., ... Woodbury, P. (2017). Natural climate solutions. *Proceedings of the National Academy of Sciences of the United States of America*, 114, 11645–11650. <https://doi.org/10.1073/pnas.1710465114>
- Halofsky, J. E., Donato, D. C., Hibbs, D. E., Campbell, J. L., Cannon, M. D., Fontaine, J. B., ... Law, B. E. (2011). Mixed-severity fire regimes: Lessons and hypotheses from the Klamath-Siskiyou Ecoregion. *Ecosphere*, 2(4), 1–9. <https://doi.org/10.1890/ES10-00184.1>
- Halpern, C. B., & Spies, T. A. (1995). Plant-species diversity in natural and managed forests of the Pacific-northwest. *Ecological Applications*, 5, 913–934. <https://doi.org/10.2307/2269343>
- Hartmann, H., Moura, C. F., Anderegg, W. R., Ruehr, N. K., Salmon, Y., Allen, C. D., ... Ruthrof, K. X. (2018). Research frontiers for improving our understanding of drought-induced tree and forest mortality. *New Phytologist*, 218, 15–28. <https://doi.org/10.1111/nph.15048>
- Hicke, J. A., Johnson, M. C., Jane, L. H. D., & Preisler, H. K. (2012). Effects of bark beetle-caused tree mortality on wildfire. *Forest Ecology and Management*, 271, 81–90. <https://doi.org/10.1016/j.foreco.2012.02.005>
- Hudiburg, T. W., Higuera, P. E., & Hicke, J. A. (2017). Fire-regime variability impacts forest carbon dynamics for centuries to millennia. *Biogeosciences*, 14, 3873–3882. <https://doi.org/10.5194/bg-14-3873-2017>
- Hudiburg, T. W., Law, B. E., & Thornton, P. E. (2013). Evaluation and improvement of the Community Land Model (CLM4) in Oregon

- forests. *Biogeosciences*, 10, 453–470. <https://doi.org/10.5194/bg-10-453-2013>
- Hudiburg, T., Law, B., Turner, D. P., Campbell, J., Donato, D. C., & Duane, M. (2009). Carbon dynamics of Oregon and Northern California forests and potential land-based carbon storage. *Ecological Applications*, 19, 163–180. <https://doi.org/10.1890/07-2006.1>
- Hudiburg, T. W., Law, B. E., Wirth, C., & Luysaert, S. (2011). Regional carbon dioxide implications of forest bioenergy production. *Nature Climate Change*, 1, 419–423. <https://doi.org/10.1038/nclimate1264>
- Hurrell, J. W., Holland, M. M., Gent, P. R., Ghan, S., Kay, J. E., Kushner, P. J., ... Lipscomb, W. H. (2013). The community earth system model a framework for collaborative research. *Bulletin of the American Meteorological Society*, 94, 1339–1360. <https://doi.org/10.1175/BAMS-D-12-00121.1>
- Jiang, X., Rauscher, S. A., Ringler, T. D., Lawrence, D. M., Williams, A. P., Allen, C. D., ... McDowell, N. G. (2013). Projected future changes in vegetation in Western North America in the twenty-first century. *Journal of Climate*, 26, 3671–3687. <https://doi.org/10.1175/JCLI-D-12-00430.1>
- Kane, J. M., & Kolb, T. E. (2014). Short- and long-term growth characteristics associated with tree mortality in southwestern mixed-conifer forests. *Canadian Journal of Forest Research*, 44, 1227–1235. <https://doi.org/10.1139/cjfr-2014-0186>
- Kelly, J. (2016). *Physiological responses to drought in healthy and stressed trees: A comparison of four species in Oregon* (64 pp). Unpublished MSc Lund University, Lund, Sweden.
- Kitzberger, T., Falk, D. A., Westerling, A. L., & Swetnam, T. W. (2017). Direct and indirect climate controls predict heterogeneous early-mid 21st century wildfire burned area across western and boreal. *North America. Plos One*, 12(12), e0188486. <https://doi.org/10.1371/journal.pone.0188486>
- Kline, J. D., Harmon, M. E., Spies, T. A., Morzillo, A. T., Pabst, R. J., McComb, B. C., ... Vogeler, J. C. (2016). Evaluating carbon storage, timber harvest, and habitat possibilities for a Western Cascades (USA) forest landscape. *Ecological Applications*, 26, 2044–2059. <https://doi.org/10.1002/eap.1358>
- Krinner, G., Viovy, N., de Noblet-Ducoudré, N., Ogée, J., Polcher, J., Friedlingstein, P., ... Prentice, I. C. (2005). A dynamic global vegetation model for studies of the coupled atmosphere-biosphere system. *Global Biogeochemical Cycles*, 19(1), <https://doi.org/10.1029/2003GB002199>.
- Lamarque, J. F., Bond, T. C., Eyring, V., Granier, C., Heil, A., Klimont, Z., ... Schultz, M. G. (2010). Historical (1850–2000) gridded anthropogenic and biomass burning emissions of reactive gases and aerosols: Methodology and application. *Atmospheric Chemistry and Physics*, 10, 7017–7039. <https://doi.org/10.5194/acp-10-7017-2010>
- Law, B. E., Hudiburg, T. W., Berner, L. T., Kent, J., Buotte, P. C., & Harmon, M. E. (2018). Land use strategies to mitigate climate change in carbon dense temperate forests. *Proceedings of the National Academy of Sciences of the United States of America*, 115, 3663–3668. <https://doi.org/10.1073/pnas.1720064115>
- Law, B. E., Thornton, P. E., Irvine, J., Anthoni, P. M., & Van Tuyl, S. (2001). Carbon storage and fluxes in ponderosa pine forests at different developmental stages. *Global Change Biology*, 7, 755–777. <https://doi.org/10.1046/j.1354-1013.2001.00439.x>
- Law, B. E., & Waring, R. H. (2015). Carbon implications of current and future effects of drought, fire and management on Pacific Northwest forests. *Forest Ecology and Management*, 355, 4–14. <https://doi.org/10.1016/j.foreco.2014.11.023>
- Levis, S., Bonan, G. B., Verstein, M., & Oleson, K. W. (2004). *The community land model's dynamic global vegetation model (CLM_DGVM): Technical description and user's guide*. In: NCAR Technical Note. Boulder, CO: National Center for Atmospheric Research.
- Li, F., Zeng, X. D., & Levis, S. (2012). A process-based fire parameterization of intermediate complexity in a Dynamic Global Vegetation Model (vol 9, pg 2761, 2012). *Biogeosciences*, 9, 4771–4772.
- Littell, J. S., Mckenzie, D., Peterson, D. L., & Westerling, A. L. (2009). Climate and wildfire area burned in western U. S. ecoprovinces, 1916–2003. *Ecological Applications*, 19, 1003–1021. <https://doi.org/10.1890/07-1183.1>
- Ma, S. Y., Baldocchi, D. D., Xu, L. K., & Hehn, T. (2007). Inter-annual variability in carbon dioxide exchange of an oak/grass savanna and open grassland in California. *Agricultural and Forest Meteorology*, 147, 157–171. <https://doi.org/10.1016/j.agrformet.2007.07.008>
- Macalady, A. K., & Bugmann, H. (2014). Growth-Mortality Relationships in Pinon Pine (*Pinus edulis*) during Severe Droughts of the Past Century: Shifting Processes in Space and Time. *Plos, One*, 9.
- McDowell, N. G., Beerling, D. J., Breshears, D. D., Fisher, R. A., Raffa, K. F., & Stitt, M. (2011). The interdependence of mechanisms underlying climate-driven vegetation mortality. *Trends in Ecology & Evolution*, 26, 523–532. <https://doi.org/10.1016/j.tree.2011.06.003>
- McDowell, N., Pockman, W. T., Allen, C. D., Breshears, D. D., Cobb, N., Kolb, T., ... Yezpe, E. A. (2008). Mechanisms of plant survival and mortality during drought: Why do some plants survive while others succumb to drought? *New Phytologist*, 178, 719–739. <https://doi.org/10.1111/j.1469-8137.2008.02436.x>
- McLauchlan, K. K., Higuera, P. E., Gavin, D. G., Perakis, S. S., Mack, M. C., Alexander, H., ... Enders, S. K. (2014). Reconstructing disturbances and their biogeochemical consequences over multiple timescales. *BioScience*, 64(2), 105–116. <https://doi.org/10.1093/biosci/bit017>
- Meddens, A. J. H., Hicke, J. A., & Ferguson, C. A. (2012). Spatiotemporal patterns of observed bark beetle-caused tree mortality in British Columbia and the western United States. *Ecological Applications*, 22, 1876–1891. <https://doi.org/10.1890/11-1785.1>
- Meigs, G. W., Campbell, J. L., Zald, H. S. J., Bailey, J. D., Shaw, D. C., & Kennedy, R. E. (2015). Does wildfire likelihood increase following insect outbreaks in conifer forests? *Ecosphere*, 6(7), art118. <https://doi.org/10.1890/ES15-00037.1>
- Mitchell, T. D., & Jones, P. D. (2005). An improved method of constructing a database of monthly climate observations and associated high-resolution grids. *International Journal of Climatology*, 25, 693–712. <https://doi.org/10.1002/joc.1181>
- Moritz, M. A., Parisien, M. A., Batllori, E., Krawchuk, M. A., Van Dorn, J., Ganz, D. J., & Hayhoe, K. (2012). Climate change and disruptions to global fire activity. *Ecosphere*, 3(6), art49. <https://doi.org/10.1890/ES11-00345.1>
- Neilson, R. P. (1993). Transient ecotone response to climatic-change - some conceptual and modeling approaches. *Ecological Applications*, 3, 385–395.
- Neilson, R. P., Pitelka, L. F., Solomon, A. M., Nathan, R., Midgley, G., Frago, J., ... Thompson, K. (2005). Forecasting regional to global plant migration in response to climate change. *BioScience*, 55, 749–759. [https://doi.org/10.1641/0006-3568\(2005\)055\[0749:FRTGPM\]2.0.CO;2](https://doi.org/10.1641/0006-3568(2005)055[0749:FRTGPM]2.0.CO;2)
- Nemani, R. R., Keeling, C. D., Hashimoto, H., Jolly, W. M., Piper, S. C., Tucker, C. J., ... Running, S. W. (2003). Climate-driven increases in global terrestrial net primary production from 1982 to 1999. *Science*, 300, 1560–1563.
- Oleson, K. W., Lawrence, D. M., Gordon, B., Flanner, M. G., Kluzek, E., Peter, J., ... Heald, C. L. (2013). *Technical description of version 4.5 of the Community Land Model (CLM)*. In: NCAR Technical Note. Boulder, CO: National Center for Atmospheric Research.
- Omernick, J. M. (2004). Perspectives on the nature and definition of ecological regions. *Environmental Management*, 34, 527–538. <https://doi.org/10.1007/s00267-003-5197-2>
- Pan, Y., Chen, J. M., Birdsey, R., Mccullough, K., He, L., & Deng, F. (2011). Age structure and disturbance legacy of North American forests. *Biogeosciences*, 8, 715–732. <https://doi.org/10.5194/bg-8-715-2011>
- Parks, S. A., Holsinger, L. M., Panunto, M. H., Jolly, W. M., Dobrowski, S. Z., & Dillon, G. K. (2018). High-severity fire: Evaluating its key drivers

- and mapping its probability across western US forests. *Environmental Research Letters*, 13(4), 044037. <https://doi.org/10.1088/1748-9326/aab791>
- Pechony, O., & Shindell, D. T. (2010). Driving forces of global wildfires over the past millennium and the forthcoming century. *Proceedings of the National Academy of Sciences of the United States of America*, 107, 19167–19170. <https://doi.org/10.1073/pnas.1003669107>
- Peters, G. P., Andrew, R. M., Boden, T., Canadell, J. G., Ciais, P., Le Quéré, C., ... Wilson, C. (2013). COMMENTARY: The challenge to keep global warming below 2 degrees C. *Nature Climate Change*, 3, 4–6.
- Raffa, K. F., Aukema, B. H., Bentz, B. J., Carroll, A. L., Hicke, J. A., Turner, M. G., & Romme, W. H. (2008). Cross-scale drivers of natural disturbances prone to anthropogenic amplification: The dynamics of bark beetle eruptions. *BioScience*, 58, 501–517. <https://doi.org/10.1641/B580607>
- Ruefenacht, B., Finco, M. V., Nelson, M. D., Czaplewski, R., Helmer, E. H., Blackard, J. A., ... Winterberger, K. (2008). Conterminous US and Alaska Forest Type Mapping Using Forest Inventory and Analysis Data. *Photogrammetric Engineering and Remote Sensing*, 74, 1379–1388. <https://doi.org/10.14358/PERS.74.11.1379>
- Rupp, D. E., Abatzoglou, J. T., Hegewisch, K. C., & Mote, P. W. (2013). Evaluation of CMIP5 20th century climate simulations for the Pacific Northwest USA. *Journal of Geophysical Research-Atmospheres*, 118, 10884–10906.
- Sala, A., Piper, F., & Hoch, G. (2010). Physiological mechanisms of drought-induced tree mortality are far from being resolved. *New Phytologist*, 186, 274–281. <https://doi.org/10.1111/j.1469-8137.2009.03167.x>
- Shafer, S. L., Bartlein, P. J., Gray, E. M., & Pellier, R. T. (2015). Projected future vegetation changes for the Northwest United States and Southwest Canada at a fine spatial resolution using a dynamic global. *Vegetation Model. Plos One*, 10. <https://doi.org/10.1371/journal.pone.0138759>
- Sitch, S., Smith, B., Prentice, I. C., Arneth, A., Bondeau, A., Cramer, W., ... Thonicke, K. (2003). Evaluation of ecosystem dynamics, plant geography and terrestrial carbon cycling in the LPJ dynamic global vegetation model. *Global Change Biology*, 9, 161–185. <https://doi.org/10.1046/j.1365-2486.2003.00569.x>
- Smith, I. A., Hutrya, L. R., Reinmann, A. B., Marrs, J. K., & Thompson, J. R. (2018). Piecing together the fragments: Elucidating edge effects on forest carbon dynamics. *Frontiers in Ecology and the Environment*, 16, 213–221. <https://doi.org/10.1002/fee.1793>
- Taylor, K. E., Stouffer, R. J., & Meehl, G. A. (2012). An overview of CMIP5 and the experiment design. *Bulletin of the American Meteorological Society*, 93, 485–498. <https://doi.org/10.1175/BAMS-D-11-00094.1>
- Thorne, J. H., Choe, H., Boynton, R. M., Bjorkman, J., Albright, W., Nydick, K., ... Schwartz, M. W. (2017). The impact of climate change uncertainty on California's vegetation and adaptation management. *Ecosphere*, 8(12). <https://doi.org/10.1002/ecs2.2021>
- Thorne, J. H., Choe, H., Stine, P. A., Chambers, J. C., Holguin, A., Kerr, A. C., & Schwartz, M. W. (2018). Climate change vulnerability assessment of forests in the Southwest USA. *Climatic Change*, 148, 387–402. <https://doi.org/10.1007/s10584-017-2010-4>
- Thornton, P. E., & Rosenbloom, N. A. (2005). Ecosystem model spin-up: Estimating steady state conditions in a coupled terrestrial carbon and nitrogen cycle model. *Ecological Modelling*, 189, 25–48. <https://doi.org/10.1016/j.ecolmodel.2005.04.008>
- van der Molen, M. K., Dolman, A. J., Ciais, P., Eglin, T., Gobron, N., Law, B. E., ... Chen, T. (2011). Drought and ecosystem carbon cycling. *Agricultural and Forest Meteorology*, 151, 765–773. <https://doi.org/10.1016/j.agrformet.2011.01.018>
- Van Mantgem, P. J., Stephenson, N. L., Byrne, J. C., Daniels, L. D., Franklin, J. F., Fulé, P. Z., ... Veblen, T. T. (2009). Widespread increase of tree mortality rates in the Western United States. *Science*, 323, 521–524. <https://doi.org/10.1126/science.1165000>
- Veblen, T. T., Hadley, K. S., Reid, M. S., & Rebertus, A. J. (1991). The response of sub-alpine forests to spruce beetle outbreak in Colorado. *Ecology*, 72, 213–231. <https://doi.org/10.2307/1938916>
- Von Arx, G., Pannatier, E. G., Thimonier, A., & Rebetez, M. (2013). Microclimate in forests with varying leaf area index and soil moisture: Potential implications for seedling establishment in a changing climate. *Journal of Ecology*, 101, 1201–1213. <https://doi.org/10.1111/1365-2745.12121>
- Waring, R. H. (1987). Characteristics of trees predisposed to die. *BioScience*, 37, 569–574. <https://doi.org/10.2307/1310667>
- Westerling, A. L., Hidalgo, H. G., Cayan, D. R., & Swetnam, T. W. (2006). Warming and earlier spring increase western US forest wildfire activity. *Science*, 313, 940–943. <https://doi.org/10.1126/science.1128834>
- Westerling, A. L., Turner, M. G., EaH, S., Romme, W. H., & Ryan, M. G. (2011). Continued warming could transform Greater Yellowstone fire regimes by mid-21st century. *Proceedings of the National Academy of Sciences of the United States of America*, 108, 13165–13170. <https://doi.org/10.1073/pnas.1110199108>
- Whittier, T. R., & Gray, A. N. (2016). Tree mortality based fire severity classification for forest inventories: A Pacific Northwest national forests example. *Forest Ecology and Management*, 359, 199–209. <https://doi.org/10.1016/j.foreco.2015.10.015>
- Williams, A. P., Allen, C. D., Macalady, A. K., Griffin, D., Woodhouse, C. A., Meko, D. M., ... Dean, J. S. (2013). Temperature as a potent driver of regional forest drought stress and tree mortality. *Nature Climate Change*, 3, 292–297. <https://doi.org/10.1038/nclimate1693>
- Wilson, B. T., Woodall, C. W., & Griffith, D. M. (2013). Imputing forest carbon stock estimates from inventory plots to a nationally continuous coverage. *Carbon Balance and Management*, 8(1), 15. <https://doi.org/10.1186/1750-0680-8-1>
- Wyckoff, P. H., & Clark, J. S. (2002). The relationship between growth and mortality for seven co-occurring tree species in the southern Appalachian Mountains. *Journal of Ecology*, 90, 604–615. <https://doi.org/10.1046/j.1365-2745.2002.00691.x>

SUPPORTING INFORMATION

Additional supporting information may be found online in the Supporting Information section at the end of the article.

How to cite this article: Buotte PC, Levis S, Law BE, Hudiburg TW, Rupp DE, Kent JJ. Near-future forest vulnerability to drought and fire varies across the western United States. *Glob Change Biol*. 2019;25:290–303. <https://doi.org/10.1111/gcb.14490>